Am J Transl Res 2019;11(1):31-44
www.ajtr.org /ISSN:1943-8141/AJTR0084577

Original Article

lncRNA GHET1 knockdown suppresses breast cancer activity in vitro and in vivo

Mingli Han[1,2], Yimeng Wang[3], Yuanting Gu[1], Xin Ge[1], Jingjing Seng[1], Guangcheng Guo[1], Xiangyu Zhang[1], Yang Zhao[1], Dongwei Dou[1,2]

[1]*Department of Breast Surgery, The First Affiliated Hospital of Zhengzhou University, Zhengzhou 450052, China;* [2]*The Key Laboratory, The First Affiliated Hospital of Zhengzhou University, Zhengzhou 450052, China;* [3]*Department of Geriatric Endocrinology, The First Affiliated Hospital of Zhengzhou University, Zhengzhou 450052, China*

Received August 25, 2018; Accepted December 18, 2018; Epub January 15, 2019; Published January 30, 2019

Abstract: Long non-coding RNA gastric carcinoma high-expressed transcript 1 (lncRNA GHET1) is highly expressed in many tumors. The aim of the present study was to determine whether GHET1 inhibition decreases growth and metastasis of MCF-7 breast cancer cells by modulating epidermal growth factor receptor (EGFR) expression. In vitro, lncRNA GHET1 knockdown suppressed cell proliferation, migration, and invasion and enhanced cell apoptosis by maintaining MCF-7 cells in the G1 phase of the cell cycle. Furthermore, lncRNA GHET1 knockdown reduced the expression of EGFR and related proteins. Treatment of mice with a GHET1 inhibitor prevented tumor growth in vivo. The results indicate that lncRNA GHET1 inhibition directly suppresses EGFR expression, significantly inhibiting the downstream PI3K/AKT/Cyclin D1/MMP2/9 pathway. This mechanism may underlie the suppression of breast cancer cell activities including proliferation, migration, and invasion. In conclusion, lncRNA GHET1 knockdown suppresses tumor growth and metastasis by suppressing the activity of EGFR and downstream pathways.

Keywords: GHET1, EGFR, proliferation, apoptosis, migration, invasion, MCF-7

Introduction

Breast cancer is one of the most common cancers worldwide and is the leading cause of cancer death among females [1]. In China, the annual incidence is growing, in part because of a "Westernized lifestyle" and exogenous estrogen [2]. Understanding the pathogenesis of this disease and finding new treatments have become important research fields.

Long non-coding RNA (lncRNA) is a class of non-coding RNA longer than 200 nucleotides [3]. lncRNA that is abundantly transcribed is of interest to many tumor researchers studying microRNA (miRNA) because of its potential roles in carcinogenesis and cancer suppression [4]. The contributions of lncRNAs to gastric cancer and their functional mechanisms remain largely unknown. Previous studies demonstrated high lncRNA GHET1 expression in gastric, colorectal, bladder, and hepatocellular cancers [5-10]. Similarly, c-Myc-encoded proteins are involved in cell proliferation, apoptosis, differentiation, and tumorigenesis [11], and c-Myc expression is elevated in some tumors [12-14]. c-Myc is also a target gene for lncRNA GHET1 in gastric cancer [15, 16]. However, the effects and mechanisms of this lncRNA and the relationship between GHET1 and c-Myc in breast cancer remain unclear. In the present study, we measured GHET1 and epidermal growth factor receptor (EGFR) expression in breast cancer and adjacent normal tissues. We also performed in vitro and in vivo experiments to evaluate the effects of lncRNA GHET1.

Materials and methods

Tissue collection

In total, 30 pairs of adjacent and tumor tissues were collected from breast cancer patient who underwent surgery at The First Affiliated Hospital of Zhengzhou University from 2014 to 2016. Among these, 15 patients were classified as Grade I and the other 15 as Grade II according to the American Joint Committee on Cancer (AJCC) TNM system. None of the

patients received preoperative radiotherapy or chemotherapy.

In situ hybridization (ISH)

After dewaxing, paraffin wax was placed in a 0.8% pepsin and hydrochloric acid mixture. The tissues were digested in a water bath for 10 min at 37°C, washed with Tris-buffered saline (TBS) for 5 min, and dried at room temperature. After 10-min ice bath annealing, the tissues were degenerated at 98°C, placed in a 37°C water bath for 1 h, and washed three times with TBS for 5 min each. A digoxin antibody labeled with alkaline phosphatase was added, and the tissues were incubated for 0.5 h at room temperature. After washing twice with BCIP/NBT under dark conditions, 0.3% nuclear fast red dye was added. The samples were stained with nitro blue tetrazolium/5-bromo-4-chloro-3-indolyl phosphate.

Immunohistochemistry (IHC)

Tumor and adjacent normal tissues were fixed with 4% neutral formaldehyde solution. Paraffin-embedded tissues were prepared as 4-μm continuous sections, and routine hematoxylin and eosin staining and IHC were performed. IHC was performed using the following conditions and procedures: paraffin dewaxing, gradient ethanol hydration citrate buffer (pH = 6.0), microwave antigen retrieval, serum blocking, overnight primary antibody addition, biotin-labeled secondary antibody incubation, streptavidin-biotin-peroxidase incubation solution addition, DAB staining, hematoxylin staining, ascending gradient alcohol dehydration, xylene addition, neutral balata usage, microscopic observations, and imaging.

Reverse transcription-polymerase chain reaction (RT-PCR)

The total RNA of adjacent and tumor tissues was extracted with a TRIzol kit (R&D, USA) according to the manufacturer's instructions. RNA concentrations were measured with a Nanodrop 2000 (Thermo Scientific, USA). RNA integrity was tested with 1% agarose gel electrophoresis, and cDNA was synthesized using a Takara reverse transcription kit with 1 μg total RNA. The sample was added on ice. The negative control for the experiment replaced the template with distilled water. Glyceraldehyde 3-phosphate dehydrogenase (GAPDH) was used as an internal control to quantify GHET1 and c-Myc levels. Gene expression was quantified with Roche's LightCycler480 (LC480) fluorescence quantitative PCR. The reaction conditions were 95°C for 30 s, followed by 95°C for 5 s, 60°C for 30 s, and 72°C for 30 s for a total of 30 cycles. Adjacent normal tissues were used as the normal control. GHET1 and c-Myc levels were measured with $2^{-\Delta\Delta Ct}$ using the following primer sequences: GHET1 F: 5'-CAACAAAGCAGGTAAACATTGG-3', R: 5'-GCAAAGGCAGAGTGAAAGGT-3'; c-Myc F: 5'-ATCACAGCCCTCACTCAC-3', R: 5'-ACAGATTCCACAAGGTGC-3'; GAPDH: F: 5'-GAACAAAGCAGGTAAACATTGG-3' and R: 5'-GACAAGCTTCCCGTTCTCAG-3'.

Cell culture

The human breast cancer cell line MCF-7 was purchased from ATCC (USA) and cultured in Dulbecco's minimum essential medium (DMEM) containing 10% fetal bovine serum (FBS) in a constant temperature incubator (37°C, 5% CO_2). Cell morphology and growth were observed daily under an inverted microscope (OLYMPUS CKX53, Japan). Cells were passaged when they reached 70%-80% confluence.

Cell grouping and treatment

The MCF-7 cells were divided into four groups: NC, normal control; BL, transfected with an empty vector; si-GHET, transfected with GHET1-shRNA (5'-CGGCAGGCATTAGAGATGAACAGCA-3'), and siGHET1+c-Myc agonist, injected with si-GHET1 and a c-Myc agonist (GenScript Co., Ltd. China).

MTT assay

Cells in the logarithmic phase of growth (2×10^3/well) were inoculated into a 96-well plate and cultured in an incubator (37°C, 5% CO_2) with normal DMEM. After 48 h, 100 μl MTT was added to the culture for 4 h. Liquid was removed, and 100 μl dimethyl sulfoxide was added. Sonication for 10 min facilitated complete crystal dissolution. Absorbance of the cells in each well was measured at 490 nm with a full wavelength multifunctional enzyme spectrometer. These data were used to calculate the cell proliferation rate in each group.

Flow cytometry

MCF-7 cells in the logarithmic proliferation phase (5×10^5 cells/well) were plated in 6-well

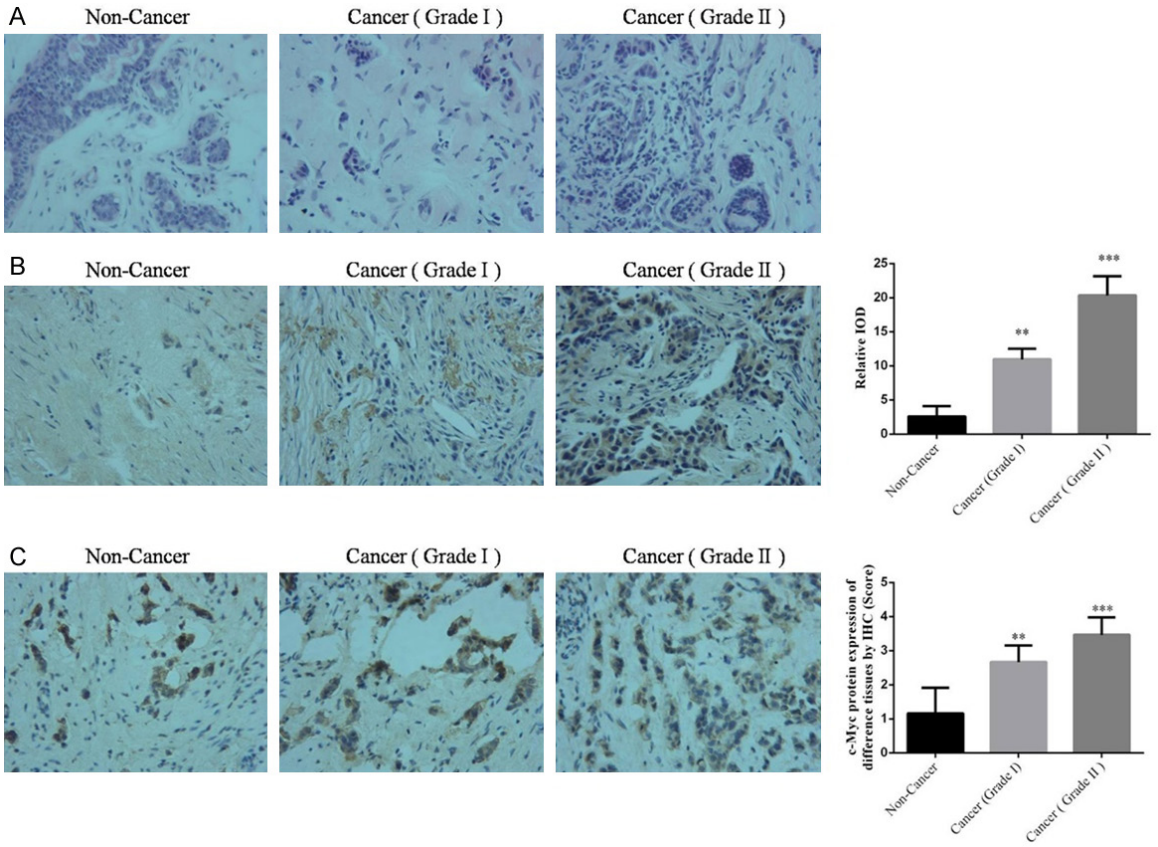

Figure 1. Tumor characteristics. A. Hematoxylin and eosin staining of non-cancer and Grade I and II breast cancer tissues (× 200). B. GHET1 expression in non-cancer and Grade I and II cancer tissues analyzed with ISH (× 200). **P < 0.05 and ***P < 0.001 vs. NC. C. c-Myc expression in non-cancer and Grade I and II cancer tissues analyzed with ISH (× 200). **P < 0.05 and ***P < 0.001 vs. NC.

plates. Cells were collected and washed three times with pre-cooled phosphate-buffered saline (PBS). After centrifugation, the supernatant was fixed with 75% ethanol at 4°C overnight. Cell cycle distribution was measured by flow cytometry. Cells were collected, washed, and suspended in PBS. Apoptosis was also evaluated by flow cytometry.

Transwell assay

MCF-7 cells from different groups (5 × 10^4 cells/well) were cultured in Transwell upper chambers. After culture, the cells were maintained for 1 h at room temperature, and serum cell suspension containing 5% calf serum albumin was added to the wells. The lower chamber was filled with 500 μL culture medium containing 10% FBS. After 48 h, the upper matrix adhesive was removed, and the lower layer was dyed with crystal violet to assess cell invasion.

Wound healing assay

MCF-7 cells (2.5 × 10^4/cm^2) were added to 6-well plates, and a scratch test was performed. The cells were cultured for 24 h. A clear straight line was made in each well with a sterile 1000-μL pipette tip, scraping the cell monolayers carefully and evenly. The cells were washed with PBS twice, and DMEM culture medium with 10% FBS was added for further incubation. Imaging was performed at 0 and 48 h.

Western blot (WB)

MCF-7 cells were collected for total protein extraction. Protein concentration was measured using the bicinchoninic acid method. The protein samples were separated with sodium dodecyl sulfate-polyacrylamide gel electrophoresis and transferred to polyvinylidene fluoride membranes. TBS-Tween contain-

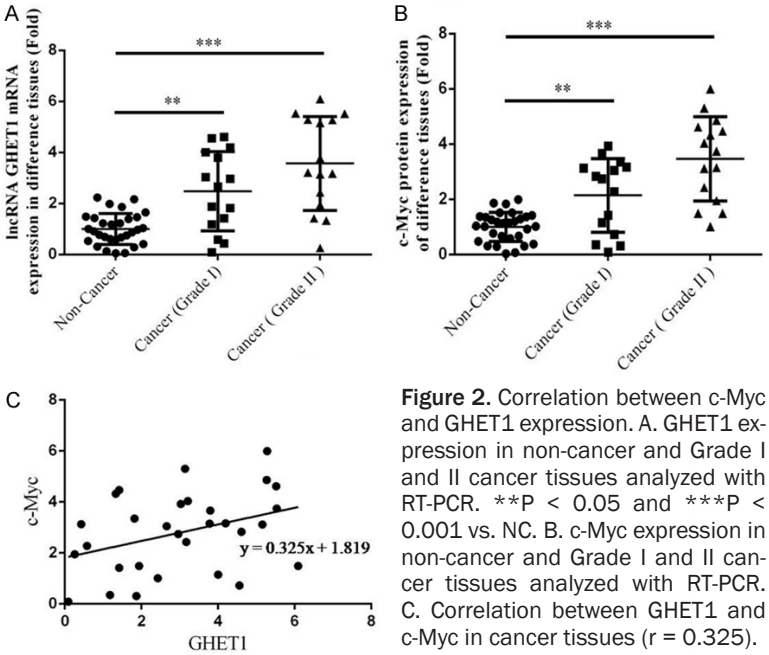

Figure 2. Correlation between c-Myc and GHET1 expression. A. GHET1 expression in non-cancer and Grade I and II cancer tissues analyzed with RT-PCR. **P < 0.05 and ***P < 0.001 vs. NC. B. c-Myc expression in non-cancer and Grade I and II cancer tissues analyzed with RT-PCR. C. Correlation between GHET1 and c-Myc in cancer tissues (r = 0.325).

ing 5% skim milk powder was applied for 2 h at room temperature to block nonspecific binding. Rabbit antibodies against human c-Myc, phosphoinositide 3-kinase (PI3K), AKT, cyclin D1, and matrix metalloproteinase (MMP)-2/9 (1:1000) were added, and the blots were incubated at 4°C overnight. After washing, horseradish peroxidase-labeled sheep anti-rabbit IgG (1:3000 dilution) was added, and the blots were incubated at room temperature for 1 h. After washing, enhanced chemiluminescence reagent was added for visualization. GAPDH was used as a loading control.

Establishment of tumor-bearing mice

Digestion was used to collect human breast cancer MCF-7 cells in the logarithmic growth phase. The cell density was adjusted to 2.0 × 10^7/mL. Each nude mouse was injected with 0.1 mL of tumor cells through the caudal vein under the armpit. The tumor-bearing mice were divided into four groups (n = 9 each): NC, BL, si-GHET1, and si-GHET1+c-Myc agonist. The NC group was injected with normal saline, BL group with an empty vector, si-GHET1 group with si-GHET1, and si-GHET1+c-Myc agonist group with si-GHET1 and a c-Myc agonist. After 30 days, the nude mice were sacrificed, and tumor volume and weight were measured for each group.

Terminal deoxynucleotidyl transferase dUTP nick end labeling (TUNEL) assay

Tumor tissue was fixed with formalin, and paraffin-embedded sections were prepared. Dewaxing was performed by placing the tissues in xylene twice for 5 min each, followed by dipping them in gradient ethanol solutions once for 3 min each. Next, 20 μg/mL protease K solution was added, and the samples were incubated at 37°C for 30 min. After washing twice with PBS, 50 μL TUNEL solution was added, and the cells were cultured at 37°C for 60 min. Cells were then washed three times in PBS and mounted on glass slides. Apoptotic cells were observed under a light microscope, and the apoptosis rate was calculated for each group.

Statistical analysis

The experimental data were processed with SSPS 13.0 statistical software (USA). The results are presented as mean ± standard deviation. Quantifiable data were evaluated with variance analysis. The Least Significant Difference test was used for comparisons between multiple groups, while comparisons between 2 groups were carried out with t-tests. P < 0.05 was considered statistically significant.

Results

Clinical data

Cell invasion was enhanced in breast cancer tissue (**Figure 1A**). ISH and IHC revealed significantly higher GHET1 and c-Myc levels in cancer tissues (**Figure 1B** and **1C**). RT-PCR showed that lncRNA GHET1 and c-Myc expression in cancer tissue were significantly upregulated compared with those in adjacent samples (both P < 0.05, **Figure 2A** and **2B**). There was a positive correlation between c-Myc and GHET1 expressions in breast cancer tissues (r = 0.325, **Figure 2C**).

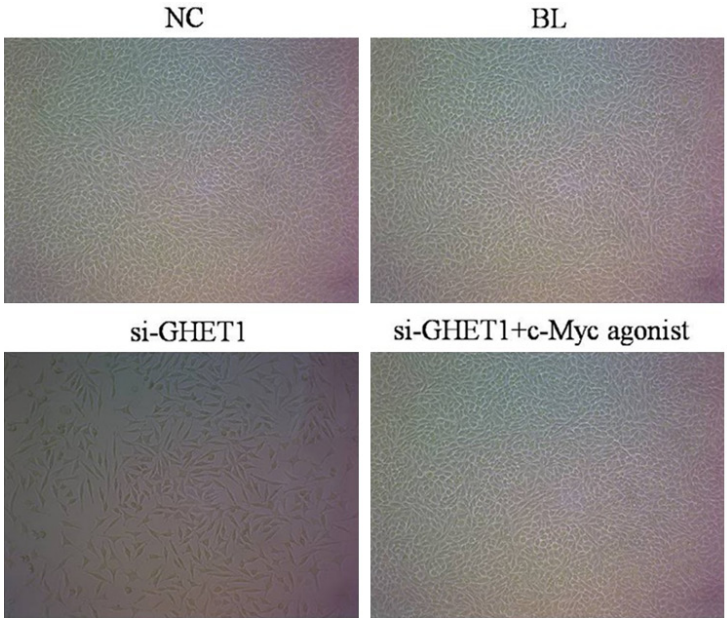

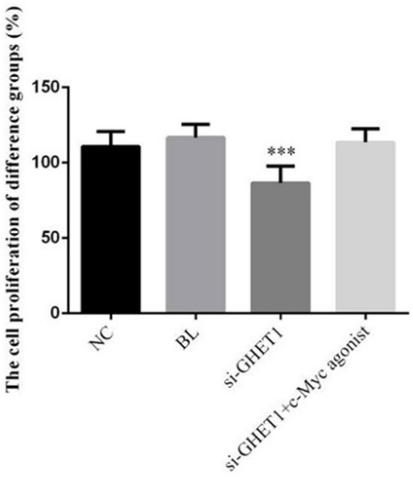

Figure 3. Cell proliferation rate in different groups analyzed with MTT assays. ***P < 0.001 vs. NC.

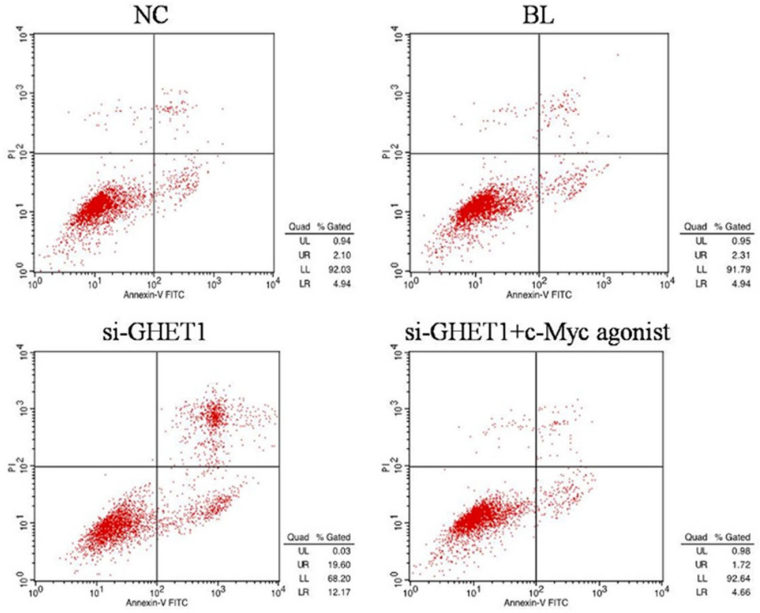

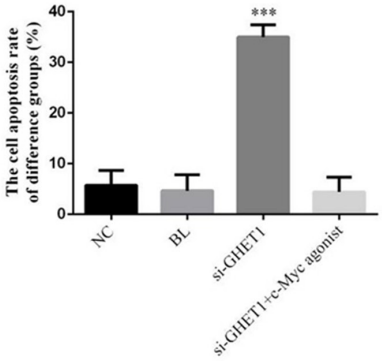

Figure 4. Apoptosis rates in different treatment groups. Flow cytometry was performed to measure cell death in control, cells transfected with empty vector (BL), and cells treated with shRNA against (si-GHET1) with or without c-Myc agonist. ***P < 0.001 vs. NC.

Cell proliferation

To investigate the effects of lncRNA GHET1 knockdown in breast cancer, we evaluated cell proliferation rates using MTT assays. The results showed a significantly lower cell proliferation rate in the si-GHET1 group compared to the NC group (P < 0.05, **Figure 3**).

Apoptosis

To evaluate the effect of lncRNA GHET1 downregulation, we performed flow cytometry to measure apoptosis in MCF-7 cells. Apoptosis in the si-GHET1 group was significantly higher compared to the NC group (P < 0.05, **Figure 4**). There were no significant differences among the NC, BL, and siGHET1+c-Myc agonist groups (P > 0.05).

Cell cycle distribution

Compared with the NC group, the G1 phase rate was significantly increased in the si-GHET1 (P < 0.05, **Figure 5**). Again, there were no significant differences among the NC, BL, and si-

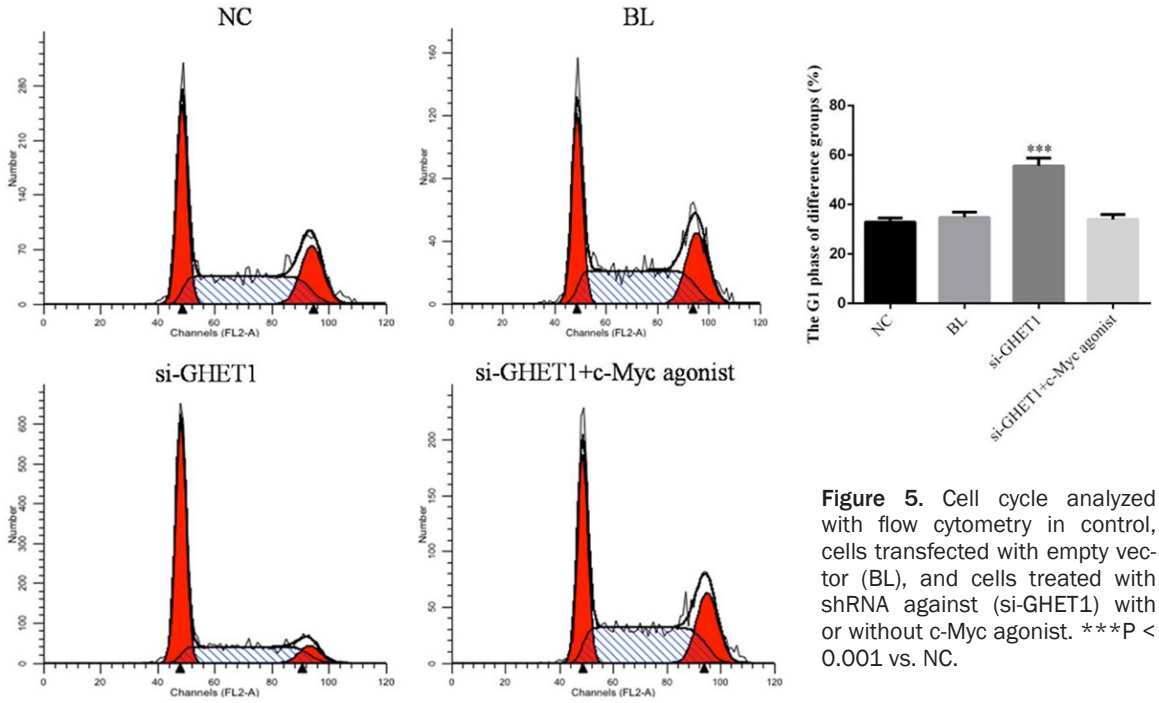

Figure 5. Cell cycle analyzed with flow cytometry in control, cells transfected with empty vector (BL), and cells treated with shRNA against (si-GHET1) with or without c-Myc agonist. ***P < 0.001 vs. NC.

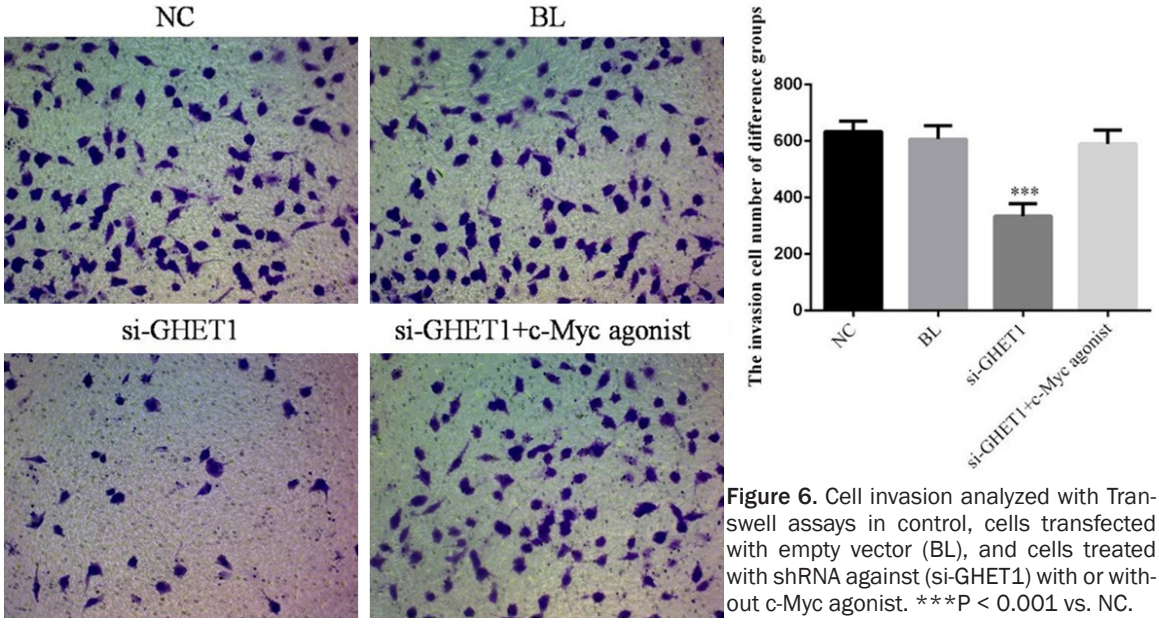

Figure 6. Cell invasion analyzed with Transwell assays in control, cells transfected with empty vector (BL), and cells treated with shRNA against (si-GHET1) with or without c-Myc agonist. ***P < 0.001 vs. NC.

GHET1+c-Myc agonist groups (P > 0.05, **Figure 5**).

Cell invasion

MCF-7 cell invasion in the si-GHET1 group was significantly lower than that in the NC group (P < 0.05, **Figure 6**). There were no significant differences among the NC, BL, and si-GHET1+c-Myc agonist groups (P > 0.05, **Figure 6**).

Cell migration

Compared with the NC group, the wound healing rate in the si-GHET1 group was significantly decreased (P < 0.05, **Figure 7**). However, there were no significant differences among the NC,

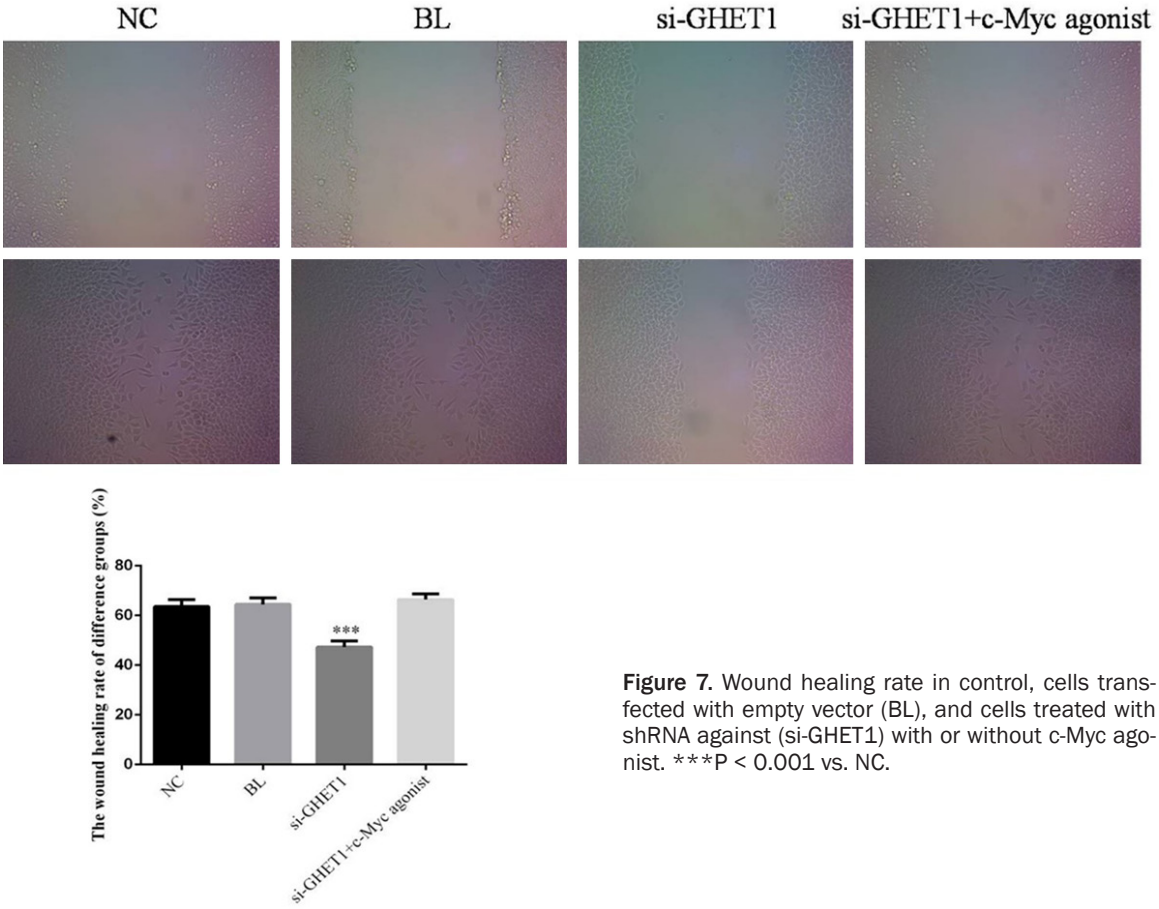

Figure 7. Wound healing rate in control, cells transfected with empty vector (BL), and cells treated with shRNA against (si-GHET1) with or without c-Myc agonist. ***P < 0.001 vs. NC.

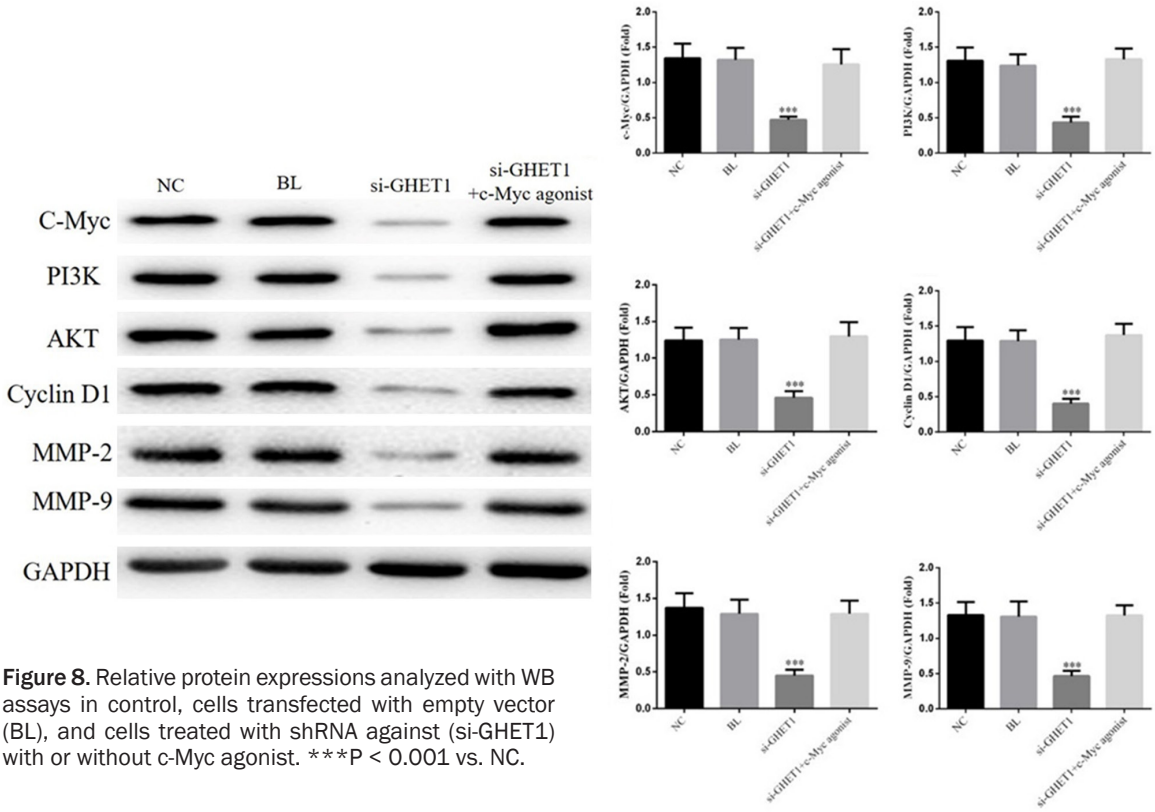

Figure 8. Relative protein expressions analyzed with WB assays in control, cells transfected with empty vector (BL), and cells treated with shRNA against (si-GHET1) with or without c-Myc agonist. ***P < 0.001 vs. NC.

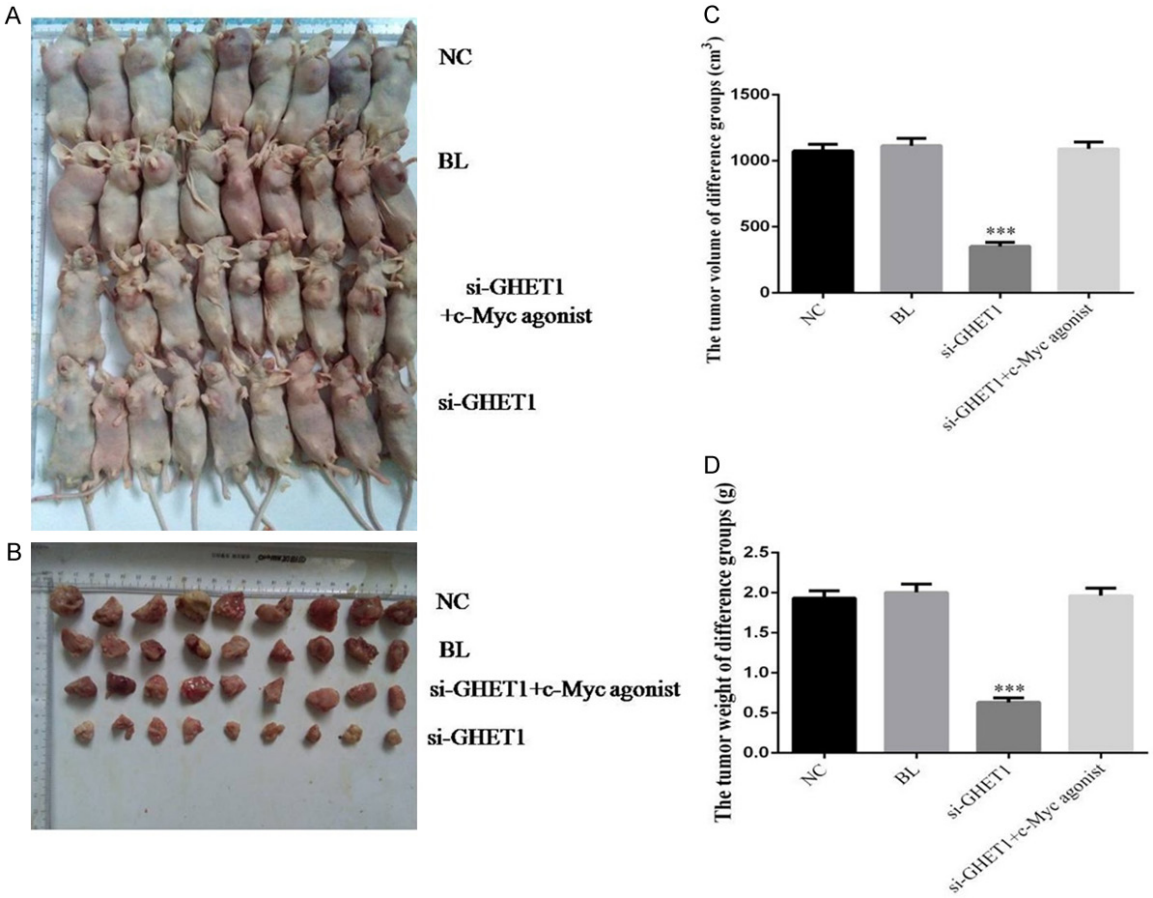

Figure 9. Tumor characteristics in each group. The NC, BL, si-GHET1, and si-GHET1+c-Myc groups were injected with normal saline, empty vector, si-GHET1, and si-GHET1+c-Myc agonist, respectively. ***P < 0.001 vs. NC. A. Tumor tissues in each group. B. Resected tumor tissues in each group. C. Analysis of tumor volumes. ***P < 0.001 vs. NC. D. Analysis of tumor weights. ***P < 0.001 vs. NC group.

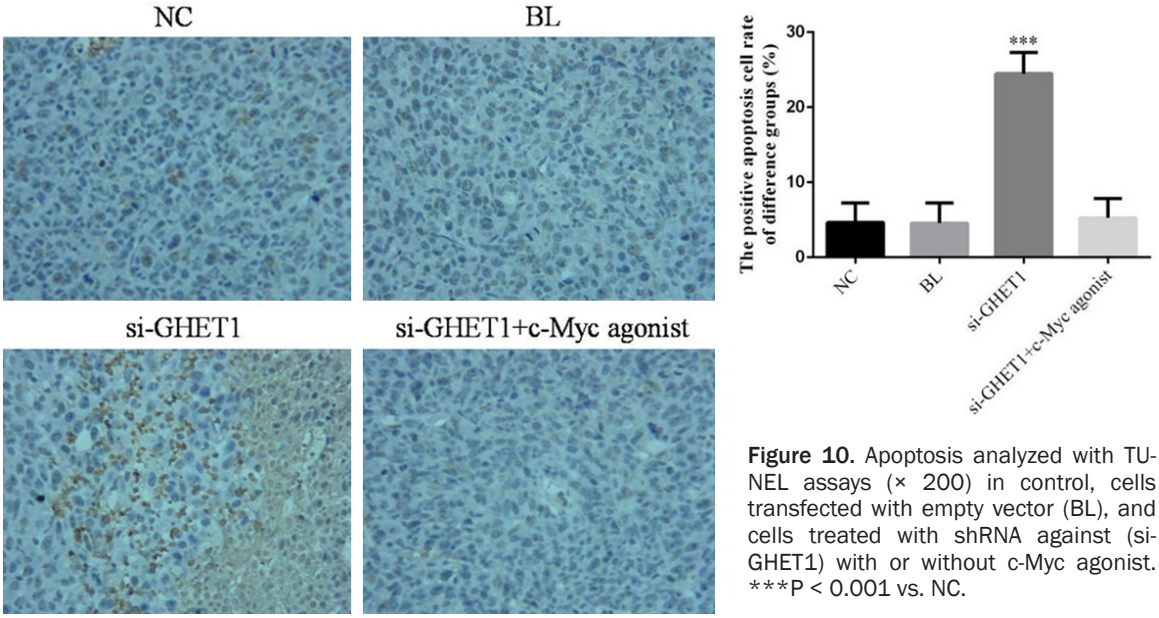

Figure 10. Apoptosis analyzed with TUNEL assays (× 200) in control, cells transfected with empty vector (BL), and cells treated with shRNA against (si-GHET1) with or without c-Myc agonist. ***P < 0.001 vs. NC.

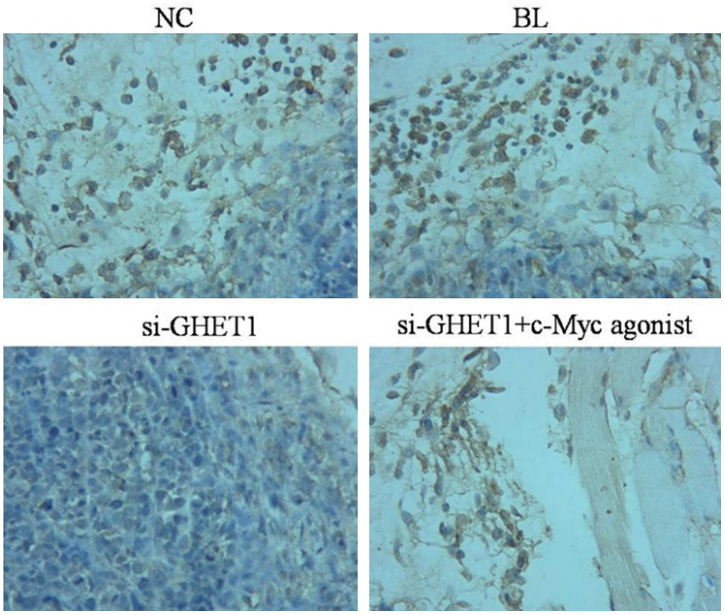

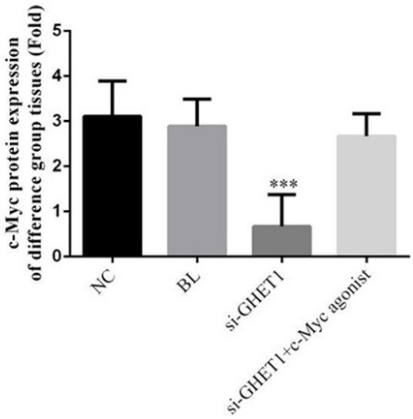

Figure 11. c-Myc expression analyzed with IHC (× 200) in control, cells transfected with empty vector (BL), and cells treated with shRNA against (si-GHET1) with or without c-Myc agonist. ***P < 0.001 vs. NC.

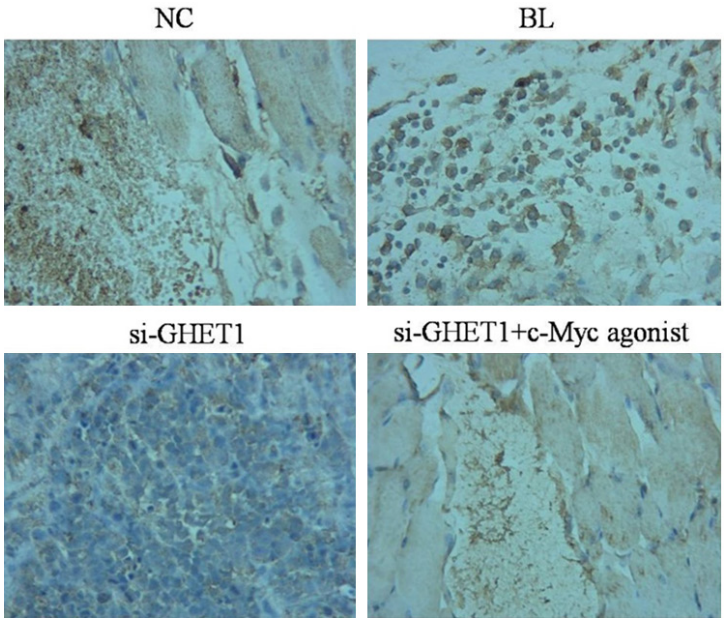

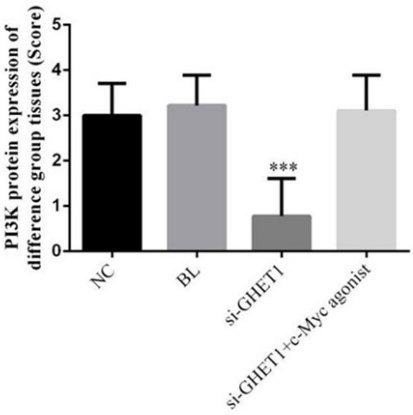

Figure 12. PI3K expression analyzed with IHC (× 200) in control, cells transfected with empty vector (BL), and cells treated with shRNA against (si-GHET1) with or without c-Myc agonist. ***P < 0.001 vs. NC.

BL, and si-GHET1+c-Myc agonist groups (P > 0.05, **Figure 7**).

Relative protein expression by WB

c-Myc, PI3K, AKT, cyclin D1, MMP-2, and -9 protein levels were significantly lower in the si-GHET1 group compared to the NC group (all P < 0.05, **Figure 8**). There were no significant differences among the NC, BL, and si-GHET1+c-Myc agonist groups in terms of c-Myc, PI3K, AKT, cyclin D1, or MMP-2 and -9 expressions (all P > 0.05, **Figure 8**).

Tumor characteristics

Compared with the NC group, the mean tumor volume and weight were significantly lower in the si-GHET1 group (P < 0.05, **Figure 9**). There were no differences among the NC, BL, and si-GHET1+c-Myc agonist groups (both P > 0.05, **Figure 9**).

Cell apoptosis

The apoptosis rate in the si-GHET1 group was significantly higher than that in the NC group (P

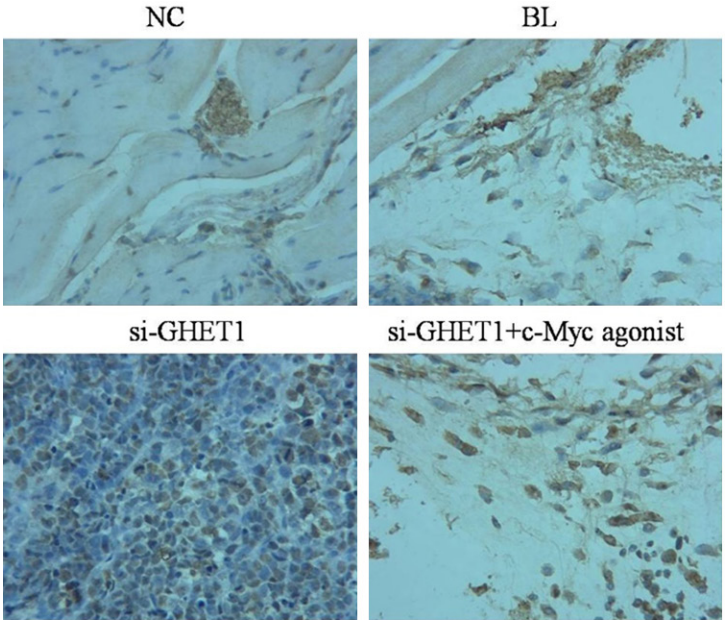

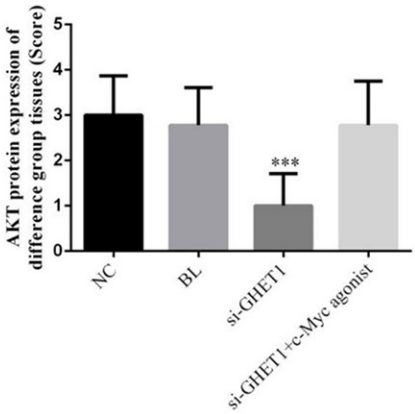

Figure 13. AKT expression analyzed with IHC (× 200) in control, cells transfected with empty vector (BL), and cells treated with shRNA against (si-GHET1) with or without c-Myc agonist. ***P < 0.001 vs. NC.

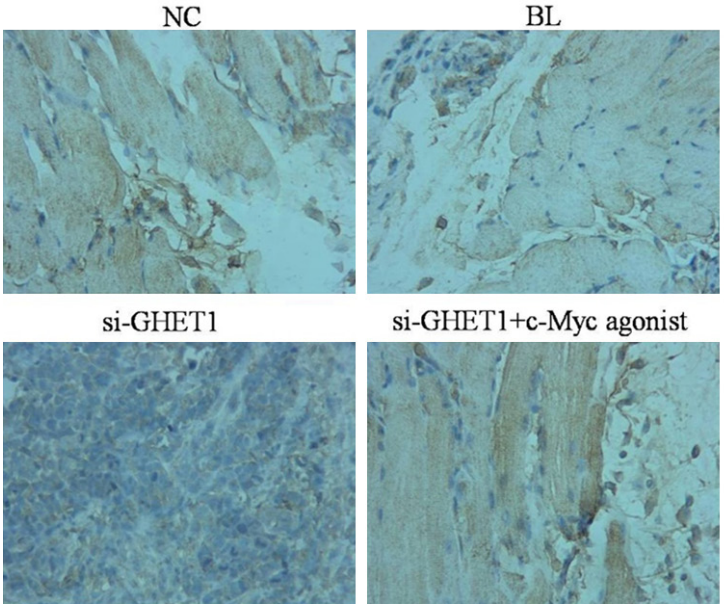

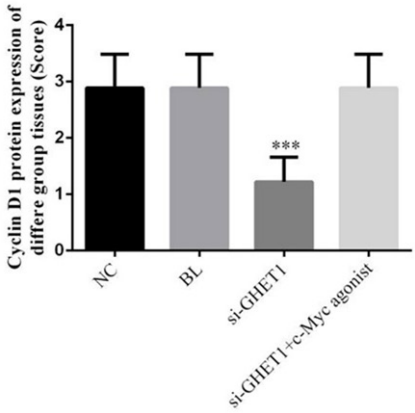

Figure 14. Cyclin D1 expression analyzed with IHC (× 200) in control, cells transfected with empty vector (BL), and cells treated with shRNA against (si-GHET1) with or without c-Myc agonist. ***P < 0.001 vs. NC.

< 0.05, **Figure 10**). However, there were no significant differences among the NC, BL, and si-GHET1+c-Myc agonist groups (all P > 0.05, **Figure 10**).

Relative protein expression by IHC

c-Myc, PI3K, AKT, cyclin D1, and MMP-2 and -9 expression in the si-GHET1 group were significantly lower than those in the NC group (P < 0.05, **Figures 11-16**). Again, there were no significant differences among the NC, BL, and si-GHET1+c-Myc agonist groups in terms of c-Myc, PI3K, AKT, cyclin D1, or MMP-2 and -9 levels (all P > 0.05, **Figures 11-16**).

Discussion

lncRNA is a class of transcribed RNA longer than 200 nucleotides [17, 18]. In humans, lncRNA accounts for most ncRNA transcripts, and the genomic distribution of lncRNA-encoding genes is very wide. Because they do not encode proteins, they were previously consid-

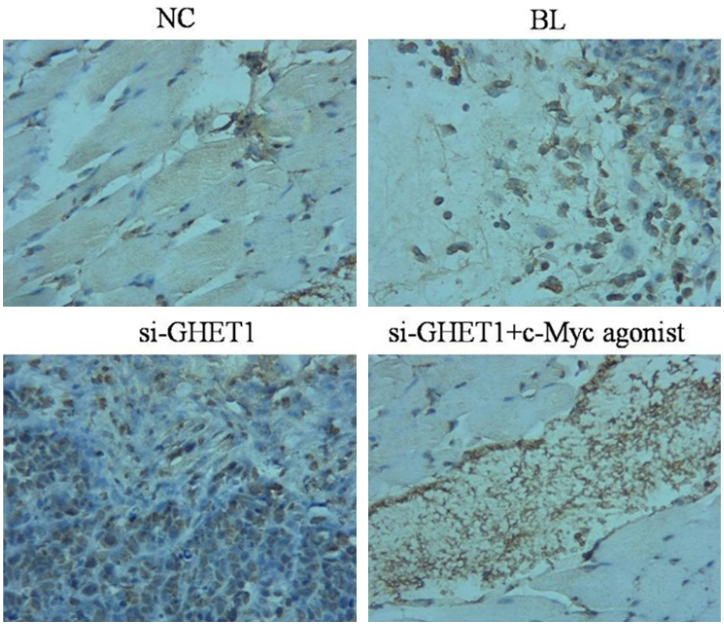

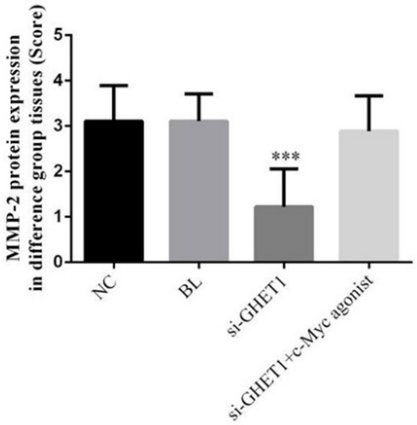

Figure 15. MMP-2 expression analyzed with IHC (× 200) in control, cells transfected with empty vector (BL), and cells treated with shRNA against (si-GHET1) with or without c-Myc agonist. ***P < 0.001 vs. NC.

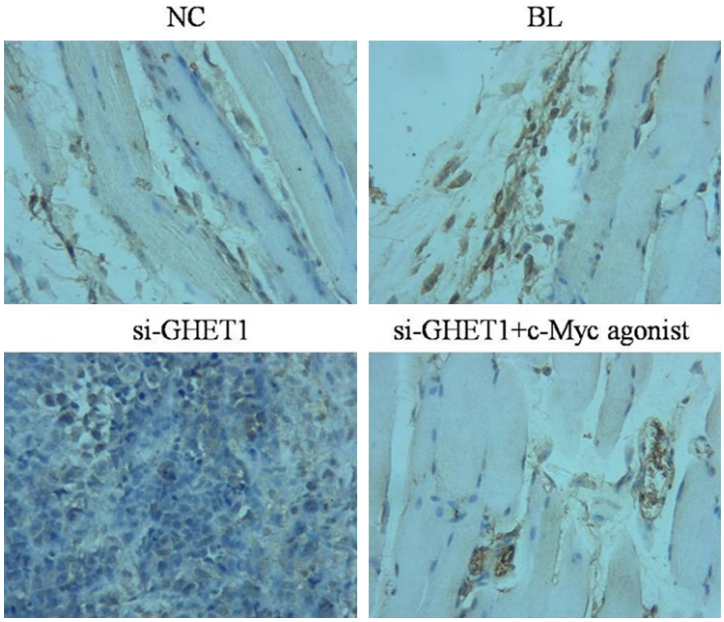

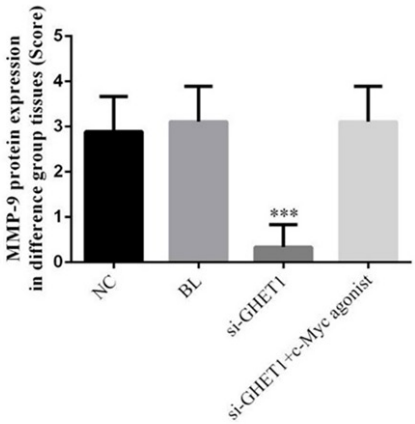

Figure 16. MMP-9 expression analyzed with IHC (× 200) in control, cells transfected with empty vector (BL), and cells treated with shRNA against (si-GHET1) with or without c-Myc agonist. ***P < 0.001 vs. NC.

ered transcription "noise." However, recent studies have shown that lncRNA plays an important role in the cellular life cycle via epigenetic modification, transcription regulation, post-transcriptional processing, translation regulation, and other mechanisms.

There are thousands of lncRNA in the human body, but < 1% of their functions are specialized. HOX transcript antisense RNA (HOTAIR) was found to contain trans-regulation lncRNA in the human chromosome 12q13.13 region. The *HOX* gene family *HOXC11* gene antisense strand, encodes a 2.2-kb long-chain non-RNA molecule that does not encode any protein. HOTAIR is upregulated in breast cancer, pancreatic cancer, hepatocellular carcinoma, and gastrointestinal stromal tumors and is closely related to tumor staging, metastasis, and survival. The present study showed that HOTAIR in conjunction with polycomb repressive complex 2 regulates histone H3 at the lysine 27th trimethylation, thus affecting p21 PTEN and WIF1 expression. These genes regulate p53, Wnt,

and Akt signaling pathways, which play important roles in the cell cycle, apoptosis, tumor angiogenesis, invasion, and metastasis [19-22]. lncRNAANRIL and lncRNA-Xist have also been implicated in regulating human cell development and tumorigenesis [23]. These lncRNAs have important roles in cancer development. Our in vitro results show that lncRNA GHET1 knockdown may suppress cell proliferation, invasion, and migration abilities and enhance cell apoptosis by increasing the G1 phase rate.

We also investigated how lncRNA GHET1 affects breast cancer development. Some previous studies [11, 15] showed that c-Myc is closely correlated with lncRNA GHET1 in gastric cancer. Our clinical data also showed positive correlations between GHET1 and c-Myc in cancer tissues. Antitumor effects of GHET1 knockdown were inhibited by a c-Myc agonist in vitro and in vivo. These results indicate that lncRNA GHET1 is related with c-Myc expression in breast cancer.

Previous studies showed that c-Myc levels are closely correlated with PI3K/AKT signaling [24-26]. The PI3K/AKT pathway has long been the focus of research on apoptosis, invasion, and migration [27-30]. The results of our study confirm that the PI3K/AKT signaling pathway is inhibited via c-Myc suppression induced by lncRNA GHET1 downregulation both in vitro and in vivo. We suggest that PI3K/AKT suppression is the mechanism underlying the lncRNA GHET1 knockdown inhibition of breast cancer activities. In the eukaryotic cell cycle, cyclin D1 is responsible for regulating the G1-to-S phase transition and cell cycle-dependent kinase protein complex formation. After the G1/S phase, cells enter the DNA synthesis S phase [31, 32]. Cyclin D1 protein expression is inhibited by PI3K/AKT suppression. This may be the mechanism underlying increased cell apoptosis due to a higher proportion of cells in G1.

MMP-2 and -9 play important roles in extracellular matrix degradation [33, 34]. This helps tumor cells infiltrate surrounding normal tissues and promotes tumor proliferation and metastasis. MMP-2 and -9 are important proteins for invasive tumor growth. In the present study, we found that MCF-7 cell invasion and migration were suppressed following lncRNA GHET1 knockout. MMP-2 and -9 levels were also decreased in the GHET1 knockout group. This suggests that lncRNA GHET1 knockdown inhibits MCF-7 cell invasion and migration abilities by suppressing MMP-2 and -9.

Collectively, our data indicate that lncRNA GHET1 knockdown directly suppresses the c-Myc and PI3K/AKT pathways. The downstream genes cyclin D1 and MMP-2/9 were also inhibited. Maintaining cells in the G1 phase leads to decreased cell proliferation, invasion, and migration and increased cell apoptosis.

Our results should be considered in the context of some limitations. The study revealed that GHET1 knockdown suppressed breast cancer cell activities via influencing upstream regulatory proteins. It still is unclear how lncRNA GHET1 levels precisely affect the expression of these proteins. We plan to explore this in future investigations.

Disclosure of conflict of interest

None.

Address correspondence to: Dongwei Dou, Department of Breast Surgery, The Key Laboratory, The First Affiliated Hospital of Zhengzhou University, Zhengzhou 450052, China. Tel: (86) 0370-67967172; Fax: (86) 0370-67967172; E-mail: 63693501@qq.com

References

[1] Santa-Maria CA, Gradishar WJ. Changing treatment paradigms in metastatic breast cancer: lessons learned. JAMA Oncol 2015; 1: 528-534.

[2] Fountzilas G, Dafni U, Papadimitriou C, Timotheadou E, Gogas H, Eleftheraki AG, Xanthakis I, Christodoulou C, Koutras A, Papandreou CN, Papakostas P, Miliaras S, Markopoulos C, Dimitrakakis C, Korantzopoulos P, Karanikiotis C, Bafaloukos D, Kosmidis P, Samantas E, Varthalitis I, Pavlidis N, Pectasides D, Dimopoulos MA. Dose-dense sequential adjuvant chemotherapy followed, as indicated, by trastuzumab for one year in patients with early breast cancer: first report at 5-year median follow-up of a Hellenic cooperative oncology group randomized phase III trial. BMC Cancer 2014; 14: 515.

[3] Liu Q, Huang J, Zhou N, Zhang Z, Zhang A, Lu Z, Wu F, Mo YY. LncRNA loc285194 is a p53-regulated tumor suppressor. Nucleic Acids Res 2013; 41: 4976-4987.

[4] Kallen AN, Zhou XB, Xu J, Qiao C, Ma J, Yan L, Lu L, Liu C, Yi JS, Zhang H, Min W, Bennett AM,

Gregory RI, Ding Y, Huang Y. The imprinted H19 lncRNA antagonizes let-7 microRNA. Mol Cell 2013; 52: 101-12.
[5] Yang F, Xue X, Zheng L, Bi J, Zhou Y, Zhi K, Gu Y, Fang G. Long non-coding RNA GHET1 promotes gastric carcinoma cell proliferation by increasing c-Myc mRNA stability. FEBS J 2014; 281: 802-813.
[6] Zhou J, Li X, Wu M, Lin C, Guo Y, Tian B. Knockdown of long noncoding RNA GHET1 inhibits cell proliferation and invasion of colorectal cancer. Oncol Res 2016; 23: 303-309.
[7] Li LJ, Zhu JL, Bao WS, Chen DK, Huang WW, Weng ZL. Long noncoding RNA GHET1 promotes the development of bladder cancer. Int J Clin Exp Pathol 2014; 7: 7196-7205.
[8] Ding G, Li W, Liu J, Zeng Y, Mao C, Kang Y, Shang J. LncRNA GHET1 activated by H3K27 acetylation promotes cell tumorigenesis through regulating ATF1 in hepatocellular carcinoma. Biomed Pharmacother 2017; 94: 326-331.
[9] Huang H, Liao W, Zhu X, Liu H, Cai L. Knockdown of long noncoding RNA GHET1 inhibits cell activation of gastric cancer. Biomed Pharmacother 2017; 92: 562-568.
[10] Zhang X, Bo P, Liu L, Zhang X, Li J. Overexpression of long non-coding RNA GHET1 promotes the development of multidrug resistance in gastric cancer cells. Biomed Pharmacother 2017; 92: 580-585.
[11] Pan XN, Chen JJ, Wang LX, Xiao RZ, Liu LL, Fang ZG, Liu Q, Long ZJ, Lin DJ. Inhibition of c-MYC overcomes cytotoxic drug resistance in acute myeloid leukemia cells by promoting differentiation. PLoS One 2014; 9: e105381.
[12] Stine ZE, Walton ZE, Altman BJ, Hsieh AL, Dang CV. MYC, metabolism, and cancer. Cancer Discov 2015; 5: 1024-1039.
[13] Dang CV. MYC on the path to cancer. Cell 2012; 149: 22-35.
[14] Khaleghian M, Shakoori A, Razavi AE, Azimi C. Relationship of amplification and expression of the C-MYC gene with survival among gastric-cancer patients. Asian Pac J Cancer Prev 2015; 16: 7061-7069.
[15] Liu H, Zhen Q, Fan Y. LncRNA GHET1 promotes esophageal squamous cell carcinoma cells proliferation and invasion via induction of EMT. Int J Biol Markers 2017; 32: e403-e408.
[16] Li T, Mo X, Fu L, Xiao B, Guo J. Molecular mechanisms of long noncoding RNAs on gastric cancer. Oncotarget 2016; 7: 8601-8612.
[17] Akhade VS, Pal D, Kanduri C. Long noncoding RNA: genome organization and mechanism of action. Adv Exp Med Biol 2017; 1008: 47-74.
[18] Jathar S, Kumar V, Srivastava J, Tripathi V. Technological developments in lncRNA biology. Adv Exp Med Biol 2017; 1008: 283-323.
[19] Zhou Y, Wang C, Liu X, Wu C, Yin H. Long noncoding RNA HOTAIR enhances radioresistance in MDA-MB231 breast cancer cells. Oncol Lett 2017; 13: 1143-1148.
[20] Yu Y, Lv F, Liang D, Yang Q, Zhang B, Lin H, Wang X, Qian G, Xu J, You W. HOTAIR may regulate proliferation, apoptosis, migration and invasion of MCF-7 cells through regulating the P53/Akt/JNK signaling pathway. Biomed Pharmacother 2017; 90: 555-561.
[21] Yang SZ, Xu F, Zhou T, Zhao X, McDonald JM, Chen Y. The long non-coding RNA HOTAIR enhances pancreatic cancer resistance to TNF-related apoptosis-inducing ligand. J Biol Chem 2017; 292: 10390-10397.
[22] Lee NK, Lee JH, Kim WK, Yun S, Youn YH, Park CH, Choi YY, Kim H, Lee SK. Promoter methylation of PCDH10 by HOTAIR regulates the progression of gastrointestinal stromal tumors. Oncotarget 2016; 7: 75307-75318.
[23] Dey BK, Mueller AC, Dutta A. Long non-coding RNAs as emerging regulators of differentiation, development, and disease. Transcription 2014; 5: e944014.
[24] Granato M, Rizzello C, Romeo MA, Yadav S, Santarelli R, D'Orazi G, Faggioni A, Cirone M. Concomitant reduction of c-Myc expression and PI3K/AKT/mTOR signaling by quercetin induces a strong cytotoxic effect against Burkitt's lymphoma. Int J Biochem Cell Biol 2016; 79: 393-400.
[25] Quan Y, Wang N, Chen Q, Xu J, Cheng W, Di M, Xia W, Gao WQ. SIRT3 inhibits prostate cancer by destabilizing oncoprotein c-MYC through regulation of the PI3K/Akt pathway. Oncotarget 2015; 6: 26494-507.
[26] Yu X, Zhen Y, Yang H, Wang H, Zhou Y, Wang E, Marincola FM, Mai C, Chen Y, Wei H, Song Y, Lyu X, Ye Y, Cai L, Wu Q, Zhao M, Hua S, Fu Q, Zhang Y, Yao K, Liu Z, Li X, Fang W. Loss of connective tissue growth factor as an unfavorable prognosis factor activates miR-18b by PI3K/AKT/C-Jun and C-Myc and promotes cell growth in nasopharyngeal carcinoma. Cell Death Dis 2013; 4: e634.
[27] Shin JA, Ryn MH, Kwon KH, Choi B, Cho SD. Down-regulation of Akt by methanol extracts of impatiens balsamina L. Promotes apoptosis in human oral squamous cell carcinoma cell lines. J Oral Pathol Med 2014; 44: 420-428.
[28] Rahmani M, Aust MM, Attkisson E, Williams DC Jr, Ferreira Gonzalez A, Grant S. Dual inhibition of Bcl-2 and Bcl-xL striking ly enhances PI3K inhibition-induced apoptosis in human myeloid leukemia cells through a GSK3- and Bim-dependent mechanism. Cancer Res 2013; 73: 1340-1351.
[29] Shan RF, Zhou YF, Peng AF, Jie ZG. Inhibition of Aurora-B suppresses HepG2 cell invasion and

migration via the PI3K/Akt/NF-κB signaling pathway in vitro. Exp Ther Med 2014; 8: 1005-1009.

[30] Zhou R, Xu L, Ye M, Liao M, Du H, Chen H. Formononetin inhibits migration and invasion of MDA-MB-231 and 4T1 breast cancer cells by suppressing MMP-2 and MMP-9 through PI3K/AKT signaling pathways. Horm Metab Res 2014; 46: 753-760.

[31] Liao K, Li J, Wang Z. Dihydroartemisinin inhibits cell proliferation via AKT/GSK3β/cyclin D1 pathway and induces apoptosis in A549 lung cancer cells. Int J Clin Exp Pathol 2014; 7: 8684-8691.

[32] Gopalakrishnan N, Saravanakumar M, Madankumar P, Thiyagu M, Devaraj H. Colocalization of β-catenin with notch intracellular domain in colon cancer: a possible role of notch1 signaling in activation of Cyclin D1-mediated cell proliferation. Mol Cell Biochem 2014; 396: 281-293.

[33] Fan SH, Wang YY, Lu J, Zheng YL, Wu DM, Zhang ZF, Shan Q, Hu B, Li MQ, Cheng W. CERS2 suppresses tumor cell invasion and is associated with decreased V-ATPase and MMP-2/MMP-9 activities in breast cancer. J Cell Biochem 2015; 116: 502-513.

[34] Yuan H, Yang P, Zhou D, Gao W, Qiu Z, Fang F, Ding S, Xiao W. Knockdown of sphingosine kinase 1 inhibits the migration and invasion of human rheumatoid arthritis fibroblast-like synoviocytes by down-regulating the PI3K/AKT activation and MMP-2/9 production in vitro. Mol Biol Rep 2014; 41: 5157-5165.